



W γ / Z γ production and New Physics constraints in ATLAS

On behalf of the ATLAS collaboration

Louis Helary – Boston University

EPS-HEP 2013

Introduction

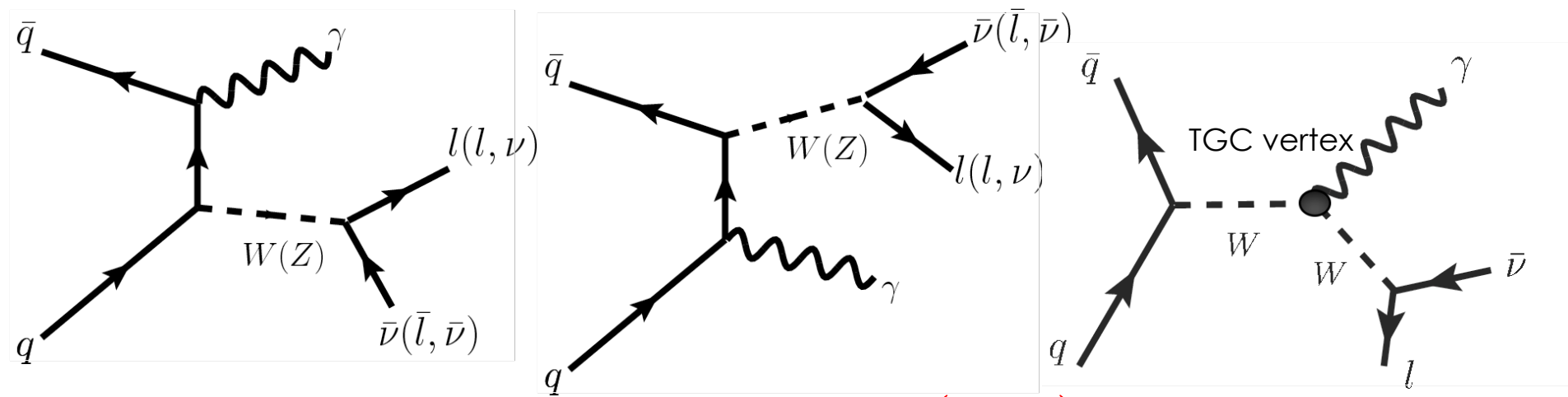
■ Studies of di-bosons final states:

- Test SM: EW and QCD predictions.
- Background in various analysis:
 - SM
 - Higgs
 - BSM
- Search for new physics:
 - Anomalous Triple Gauge Coupling (aTGC).
 - Resonant excess.

“Measurements of $W \gamma$ and $Z \gamma$ production in pp collisions at $\sqrt{s} = 7$ TeV with the ATLAS detector at the LHC”

Phys. Rev. D 87, 112003 (2013)

■ Three processes studied with the full 2011 dataset ($L=4.6 \text{ fb}^{-1}$): $(l \nu \gamma)$, $(ll \gamma)$, $(\nu \nu \gamma)$.



$W(l\nu)\gamma$

■ Selection:

- 1 good lepton:
 - $p_T^l > 25$ GeV.
- $E_T^{\text{Miss}} > 35$ GeV.
- 1 isolated photon:
 - $E_T > 15$ GeV.

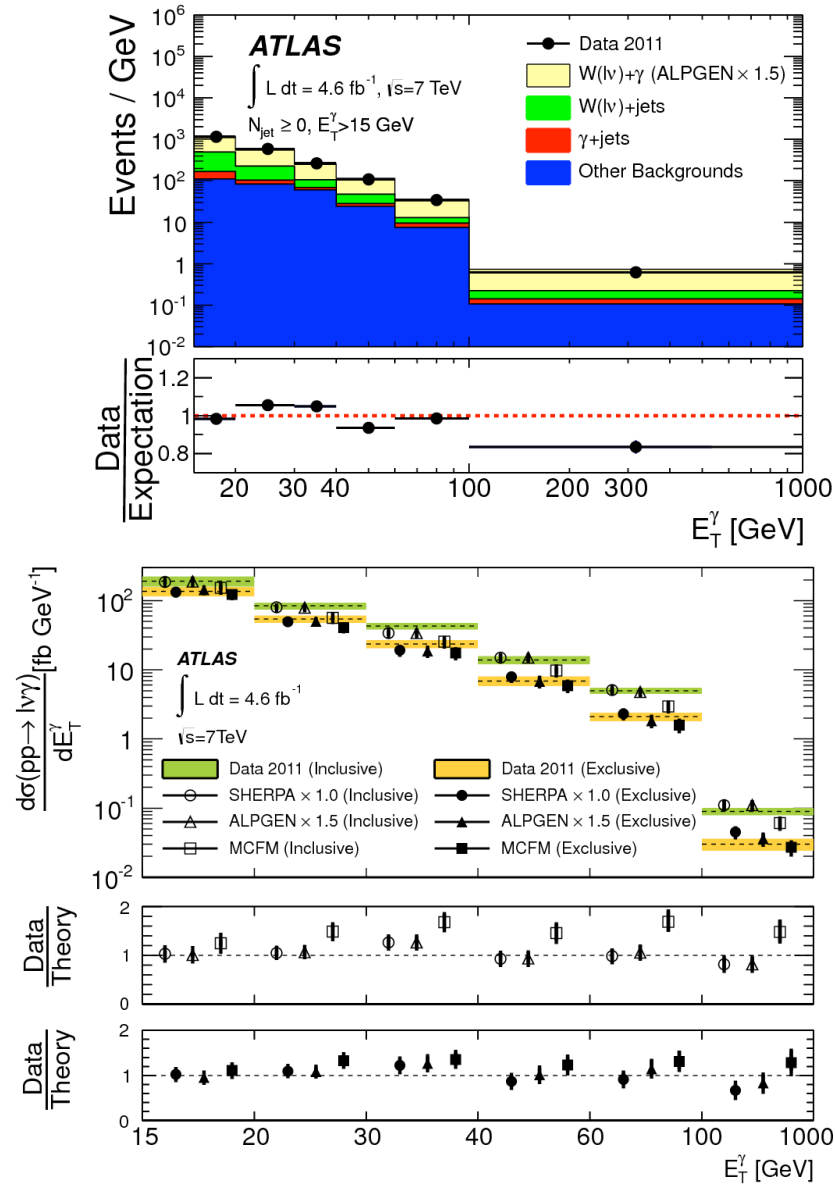
■ Differential E_T^γ measurement:

- AlpGen and Sherpa describe the shape properly.
- Comparison to MCFM NLO prediction:
 - Disagreement in high E_T^γ for $N_{\text{jet}} \geq 0$.
 - Agreement improved for $N_{\text{jet}} = 0$.

■ More:

- Inclusive ($N_{\text{jet}} \geq 0$) & exclusive ($N_{\text{jet}} = 0$) σ measurement.
- Jet multiplicity unfolding.
- Three body transverse mass unfolding.

Louis Helary - Boston University



$Z(\ell\ell)\gamma$

■ Selection:

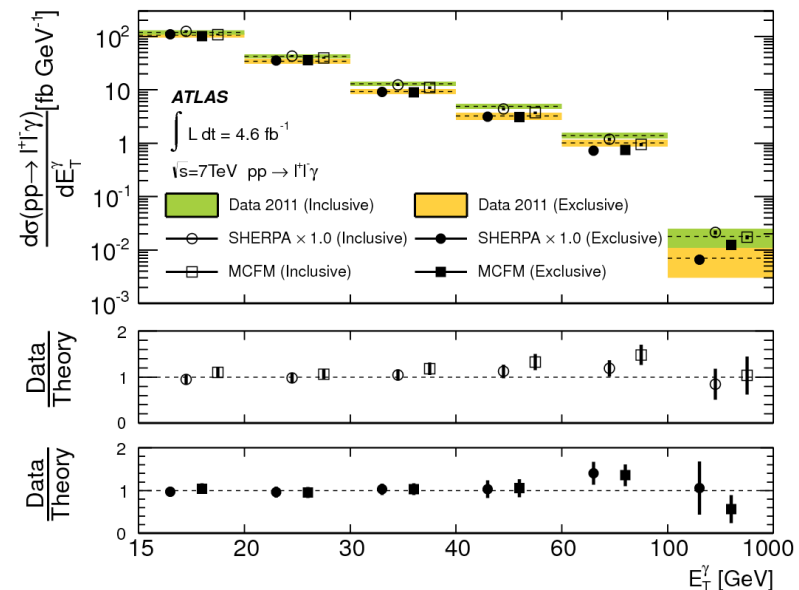
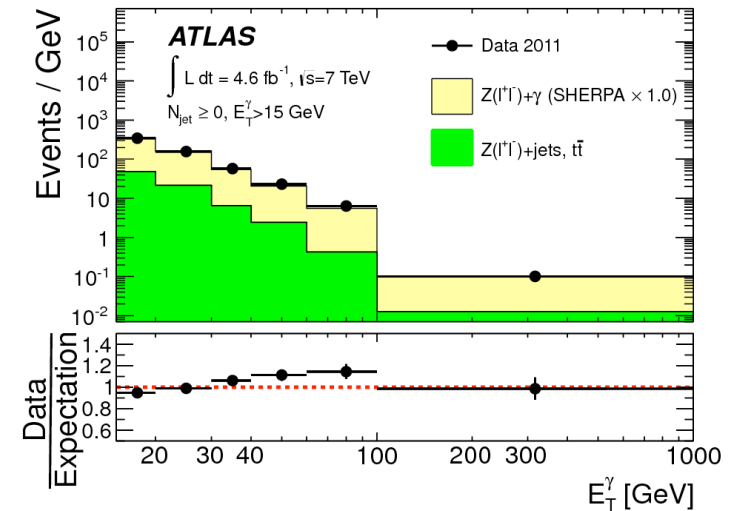
- 2 good leptons:
 - $p_T^\ell > 25$ GeV.
 - $m^{\ell\ell} > 40$ GeV.
- 1 isolated photon:
 - $E_T^\gamma > 15$ GeV.

■ Differential E_T^γ measurement:

- Sherpa describe the shape properly.
- Fair agreement with MCFM NLO predictions.
- First ATLAS differential measurement for $Z(\ell\ell)\gamma$!

■ More:

- Inclusive ($N_{\text{jet}} \geq 0$) & exclusive ($N_{\text{jet}} = 0$) σ measurement.
- Jet multiplicity unfolding.
- Three body invariant mass unfolding.



$Z(\nu\nu)\gamma$

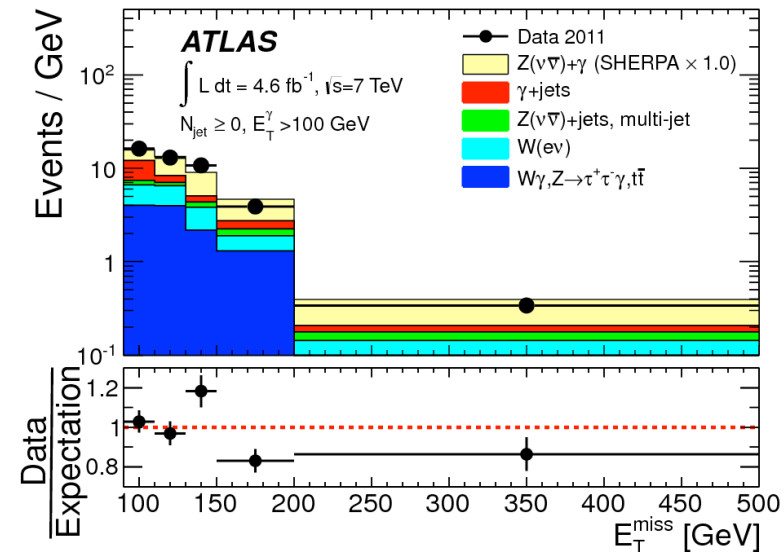
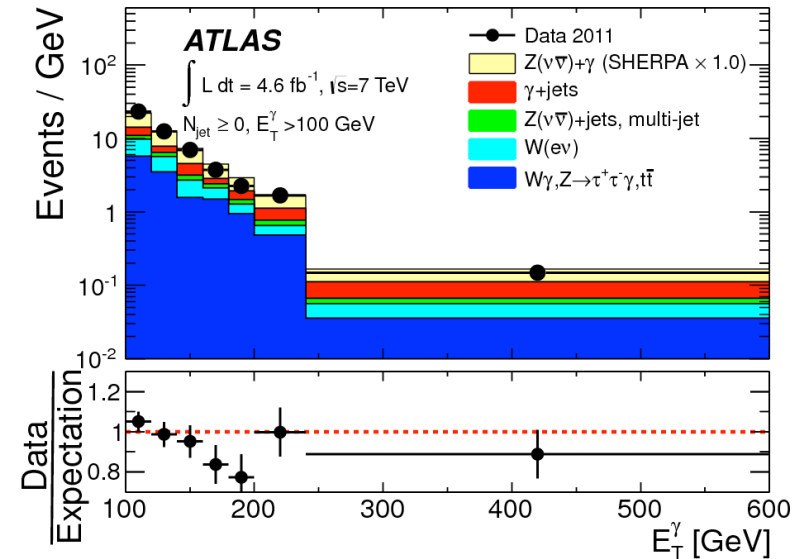
Selection:

- 0 good leptons.
- $E_T^{\text{Miss}} > 90$ GeV.
- 1 isolated photon:
 - $E_T > 100$ GeV.

Inclusive and exclusive σ measurement:

- First ATLAS measurement for $Z(\nu\nu)\gamma$!

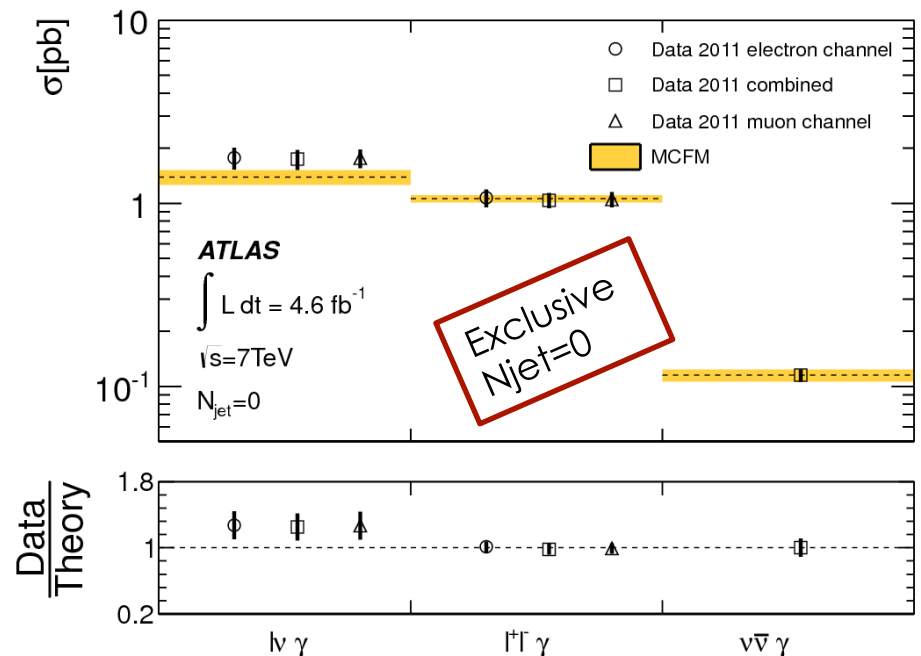
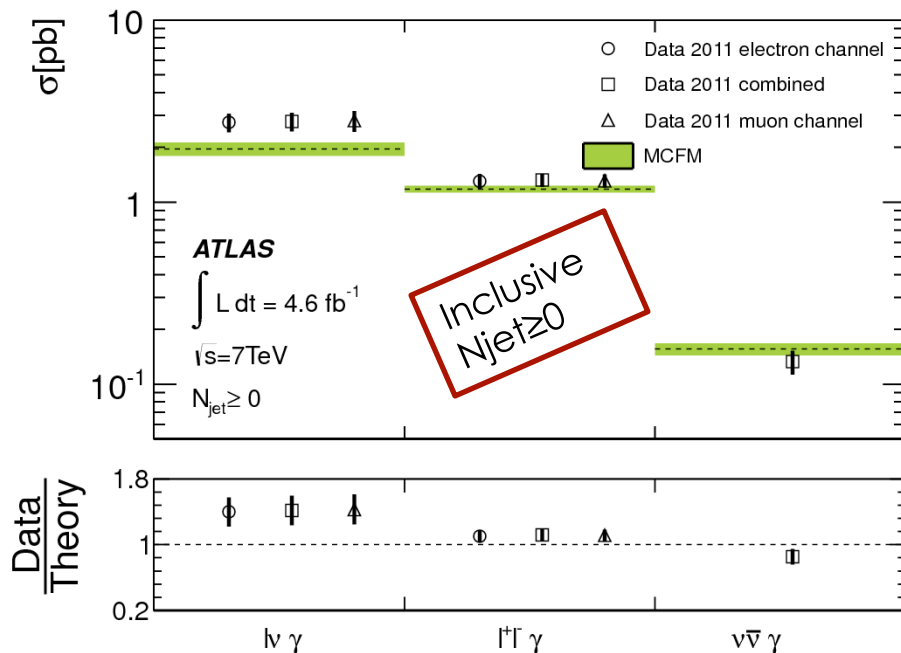
	$\nu\bar{\nu}\gamma$ $N_{\text{jet}} \geq 0$	$\nu\bar{\nu}\gamma$ $N_{\text{jet}} = 0$
$N_{Z\gamma}^{\text{obs}}$	1094	662
$W(\nu\bar{\nu})$	$171 \pm 2 \pm 17$	$132 \pm 2 \pm 13$
$Z(\nu\bar{\nu})+\text{jets, multi-jet}$	$70 \pm 13 \pm 14$	$29 \pm 5 \pm 3$
$W\gamma$	$238 \pm 12 \pm 37$	$104 \pm 9 \pm 24$
$\gamma+\text{jets}$	$168 \pm 20 \pm 42$	$26 \pm 7 \pm 11$
$Z(\tau^+\tau^-)\gamma$	$11.7 \pm 0.7 \pm 0.9$	$6.5 \pm 0.6 \pm 0.6$
$t\bar{t}$	$11 \pm 1.2 \pm 1.0$	$0.9 \pm 0.6 \pm 0.1$
$N_{Z\gamma}^{\text{sig}}$	$420 \pm 42 \pm 60$	$360 \pm 29 \pm 30$



Integrated cross section measurement

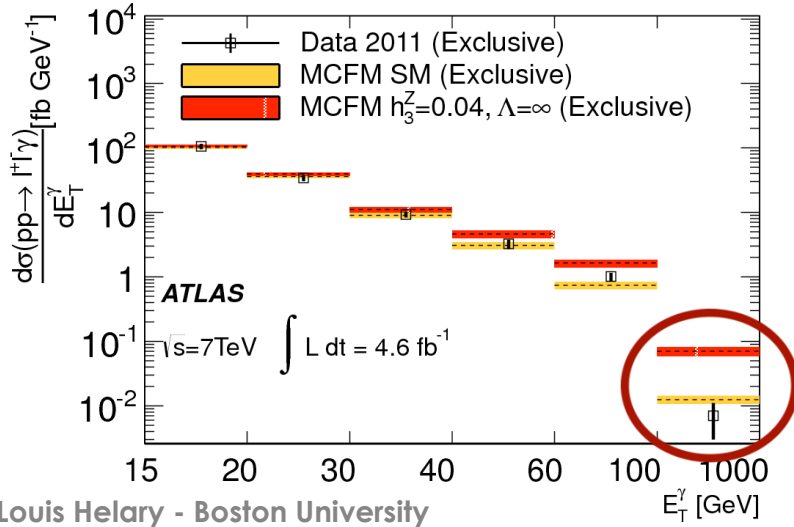
Measurement compared to MCFM NLO predictions.

- Good agreement for $Z \gamma$.
- Worse agreement for $W \gamma$.
 - 2σ above predictions for $N_{\text{jet}} \geq 0$.
 - Agreement improved for $N_{\text{jet}} = 0$.



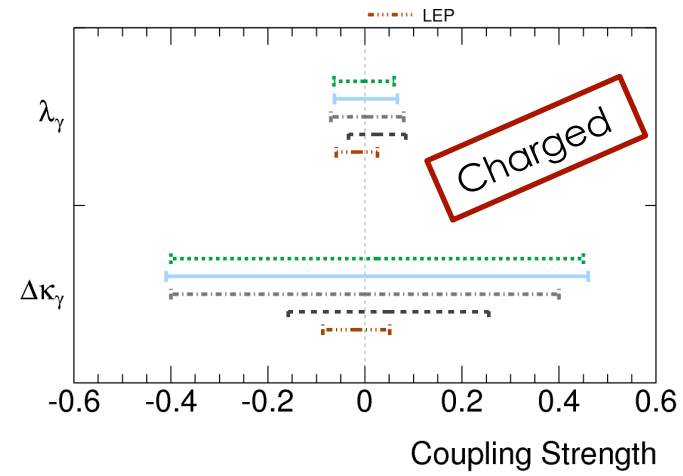
Anomalous Triple Gauge Coupling

- s-channel diagram contains TGC vertex.
 - Forbidden for $Z \gamma$ final state.
 - aTGC: Enhanced cross section at high energy.
 - Use 2D effective parameterization of each coupling.
- Search for aTGC using exclusive ($N_{jet}=0$) photon E_T in $Z(l\bar{l}) \gamma$, $Z(\nu \bar{\nu}) \gamma$ and $W(l \nu) \gamma$ final state.
- No significant deviations from the SM predictions.
- Limits comparable or better to that obtained at Tevatron and LEP.

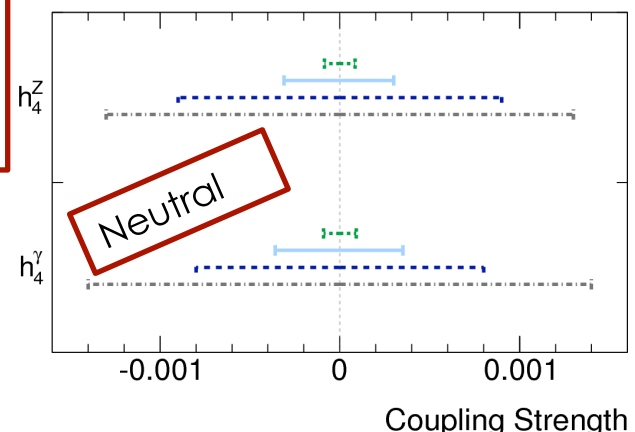


Use last $E_T \gamma$ bin to extract aTGC limits

ATLAS \cdots ATLAS, $\sqrt{s} = 7 \text{ TeV}$ \cdots D0 ($W\gamma$), $\sqrt{s} = 1.96 \text{ TeV}$
 $pp \rightarrow l\nu \gamma$ $4.6 \text{ fb}^{-1}, \Lambda = \infty$ $4.2 \text{ fb}^{-1}, \Lambda = 2 \text{ TeV}$
 95% CL --- ATLAS, $\sqrt{s} = 7 \text{ TeV}$ --- D0 ($WW, WZ, W\gamma$), $\sqrt{s} = 1.96 \text{ TeV}$
 $4.6 \text{ fb}^{-1}, \Lambda = 6 \text{ TeV}$ $8.6 \text{ fb}^{-1}, \Lambda = 2 \text{ TeV}$

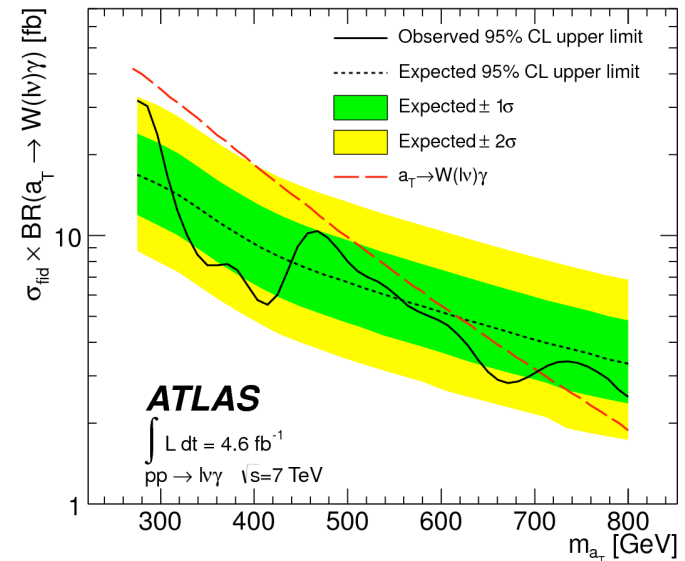
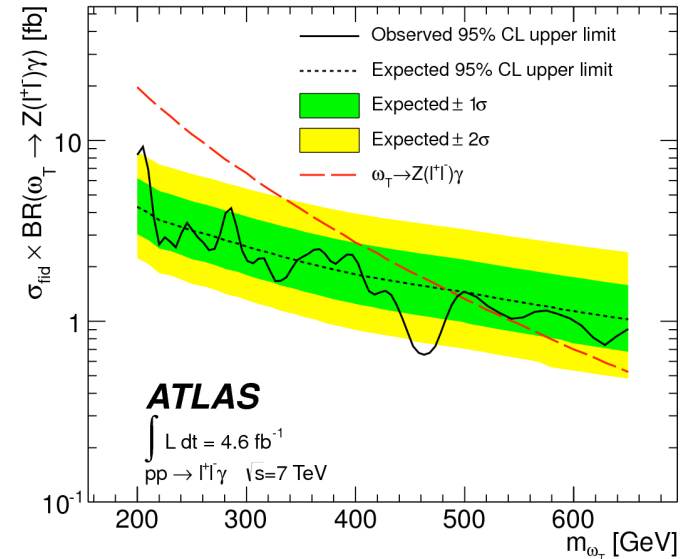
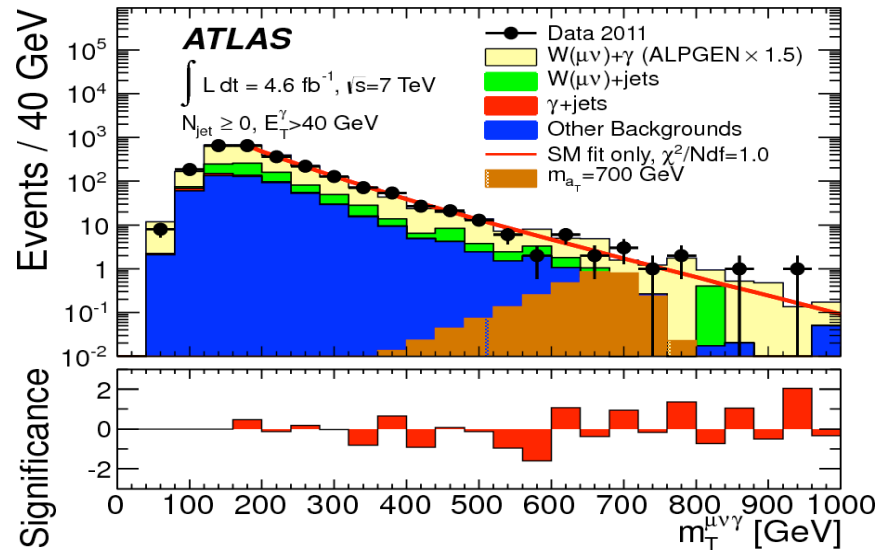


ATLAS \cdots ATLAS, $\sqrt{s} = 7 \text{ TeV}$ \cdots CDF, $\sqrt{s} = 1.96 \text{ TeV}$
 $pp \rightarrow l^+l^-\gamma, pp \rightarrow \nu\bar{\nu}\gamma$ $4.6 \text{ fb}^{-1}, \Lambda = \infty$ $5.1 \text{ fb}^{-1}, \Lambda = 1.5 \text{ TeV}$
 95% CL --- ATLAS, $\sqrt{s} = 7 \text{ TeV}$ --- D0, $\sqrt{s} = 1.96 \text{ TeV}$
 $4.6 \text{ fb}^{-1}, \Lambda = 3 \text{ TeV}$ $7.2 \text{ fb}^{-1}, \Lambda = 1.5 \text{ TeV}$



BSM Search

- Use 3 body transverse mass ($W \gamma$) and invariant mass ($Z \gamma$) to search for a resonant excess.
- Obtain model independent limits on $W \gamma$ and $Z \gamma$ $\sigma \times BR$ production.
 - Use Low Scale Technicolor (LSTC) as a benchmark:
 - $a_T \rightarrow W \gamma$: $M(a_T) = 703 \text{ GeV}$.
 - $\omega_T \rightarrow Z \gamma$: $M(\omega_T) = 494 \text{ GeV}$.
- First limit published on $W(l \nu) \gamma$ final state!
- Best limit published on $Z(l l) \gamma$ final state!



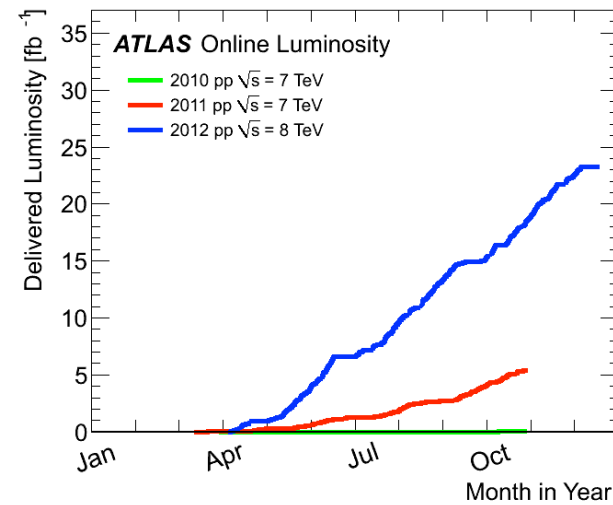
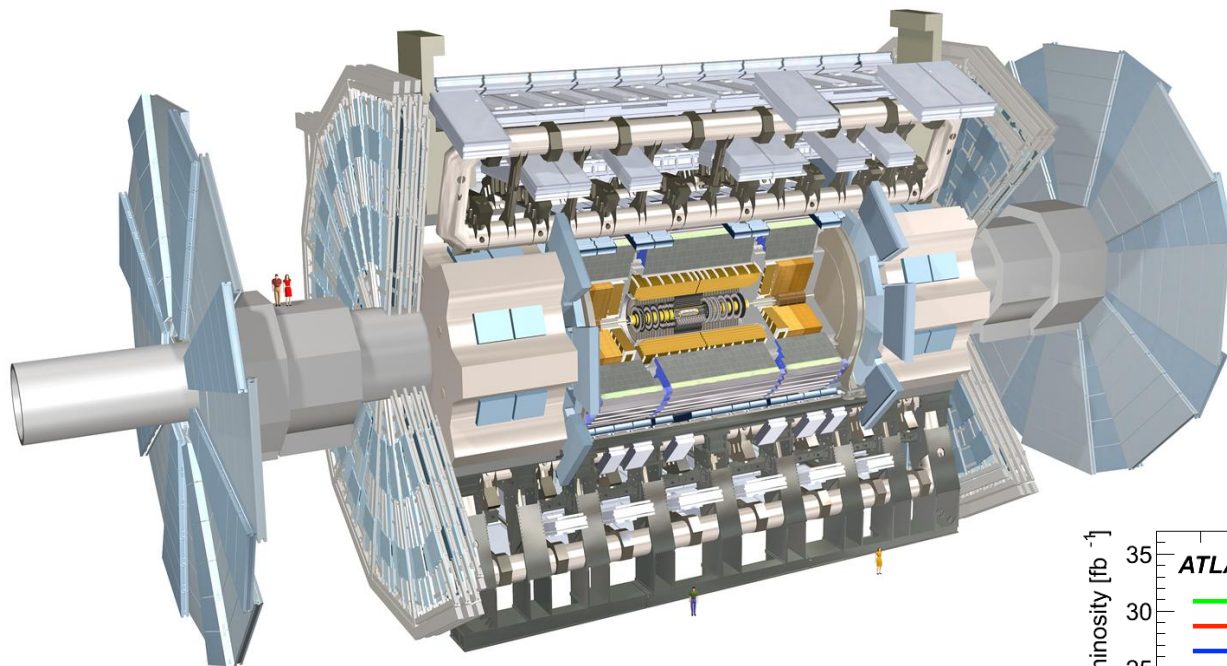
Conclusions

- **ATLAS 7 TeV ($V \gamma$) results were presented.**
- **Integrated cross-section:**
 - Good agreement with NLO predictions found for $Z \gamma$.
 - 2σ agreement for $W \gamma$.
 - Improvement for $N_{\text{jets}}=0$.
- **Differential cross-section:**
 - Discrepancies with NLO predictions for high E_T^γ in $W \gamma$.
 - Shapes properly described by multi-leg generator: AlpGen, Sherpa.
- **Search for New Physics:**
 - aTGC:
 - Limits are comparable to Tevatron or LEP results.
 - Narrow resonance search:
 - First published narrow resonance search in $W \gamma$!
 - Best published limit for narrow resonance search in $Z \gamma$!
- **No obvious sign of new physics...**

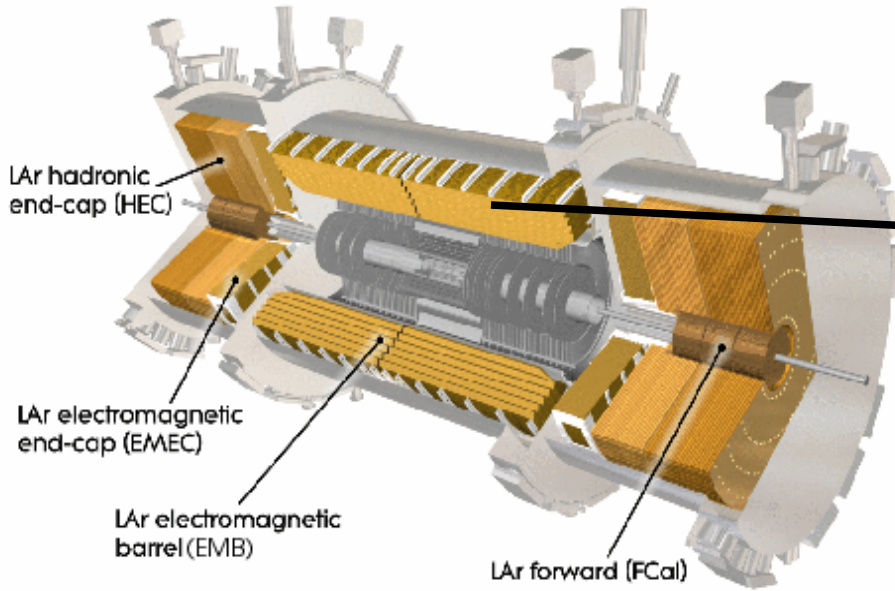


Back-up

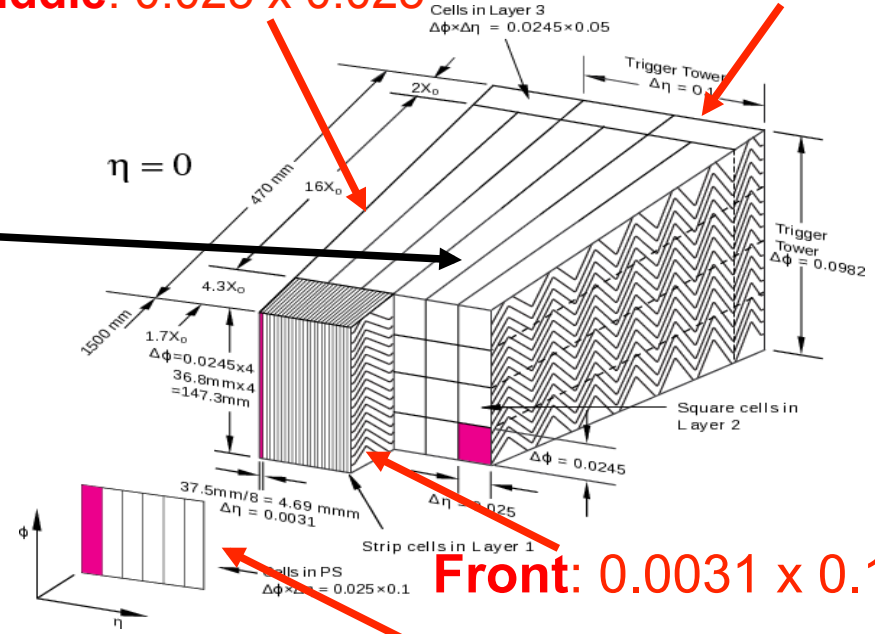
ATLAS & Lumi



Calorimeter

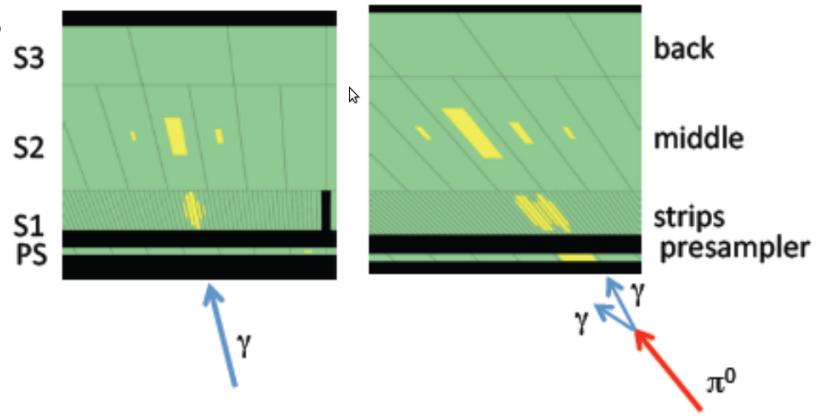


Back: 0.05 x 0.025
middle: 0.025 x 0.025



Front: 0.0031 x 0.1
PS: 0.025 x 0.1

Why this granularity?



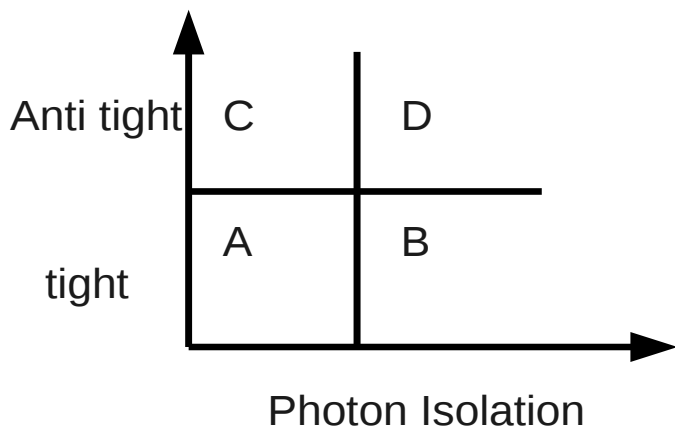
Background decomposition

	$e\nu\gamma$		$\mu\nu\gamma$	
	$N_{\text{jet}} \geq 0$		$N_{\text{jet}} = 0$	
$N_{W\gamma}^{\text{obs}}$	7399		10914	
$W(\ell\nu)+\text{jets}$	$1240 \pm 160 \pm 210$	$2560 \pm 270 \pm 580$	$910 \pm 160 \pm 160$	$1690 \pm 210 \pm 270$
$Z(\ell^+\ell^-) + X$	$678 \pm 18 \pm 86$	$779 \pm 19 \pm 93$	$411 \pm 13 \pm 51$	$577 \pm 16 \pm 73$
$\gamma+\text{jets}$	$625 \pm 80 \pm 86$	$184 \pm 9 \pm 15$	$267 \pm 79 \pm 54$	$87 \pm 7 \pm 14$
$t\bar{t}$	$320 \pm 8 \pm 28$	$653 \pm 11 \pm 57$	$22 \pm 2 \pm 4$	$44 \pm 3 \pm 6$
other background	$141 \pm 16 \pm 13$	$291 \pm 29 \pm 26$	$52 \pm 5 \pm 6$	$140 \pm 22 \pm 18$
$N_{W\gamma}^{\text{sig}}$	$4390 \pm 200 \pm 250$		$6440 \pm 300 \pm 590$	

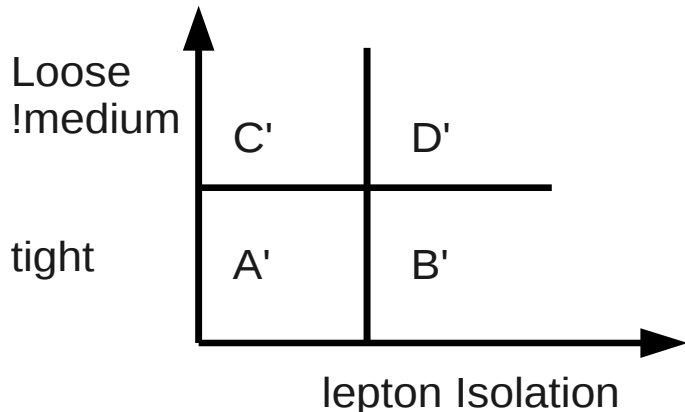
	$e^+e^-\gamma$		$\mu^+\mu^-\gamma$	
	$N_{\text{jet}} \geq 0$		$N_{\text{jet}} = 0$	
$N_{Z\gamma}^{\text{obs}}$	1908		2756	
$N_{Z\gamma}^{\text{BG}}$	$311 \pm 57 \pm 68$	$366 \pm 83 \pm 73$	1417	2032
$N_{Z\gamma}^{\text{sig}}$	$1600 \pm 71 \pm 68$	$2390 \pm 97 \pm 73$	$1260 \pm 56 \pm 32$	$1790 \pm 59 \pm 49$

	$\nu\bar{\nu}\gamma$	$\nu\bar{\nu}\gamma$
	$N_{\text{jet}} \geq 0$	$N_{\text{jet}} = 0$
$N_{Z\gamma}^{\text{obs}}$	1094	662
$W(e\nu)$	$171 \pm 2 \pm 17$	$132 \pm 2 \pm 13$
$Z(\nu\bar{\nu})+\text{jets, multi-jet}$	$70 \pm 13 \pm 14$	$29 \pm 5 \pm 3$
$W\gamma$	$238 \pm 12 \pm 37$	$104 \pm 9 \pm 24$
$\gamma+\text{jets}$	$168 \pm 20 \pm 42$	$26 \pm 7 \pm 11$
$Z(\tau^+\tau^-\gamma)$	$11.7 \pm 0.7 \pm 0.9$	$6.5 \pm 0.6 \pm 0.6$
$t\bar{t}$	$11 \pm 1.2 \pm 1.0$	$0.9 \pm 0.6 \pm 0.1$
$N_{Z\gamma}^{\text{sig}}$	$420 \pm 42 \pm 60$	$360 \pm 29 \pm 30$

2D sideband



+



Normalization:

$$N_A^{Wjet} = N_A - N_A^{EWbkg} - (N_A^{W\gamma} + N_A^{\gamma jet}) = N_A - N_A^{EWbkg} - \frac{E * (-1 + \sqrt{1+F})}{G}$$

$$N_A^{\gamma jet} = N_A - N_A^{EWbkg} - (N_A^{W\gamma} + N_A^{Wjet}) = N_A - N_A^{EWbkg} - \frac{E' * (-1 + \sqrt{1+F'})}{G'}$$

$$N_A^{W\gamma} = N_A - N_A^{EWbkg} - N_A^{\gamma jet} - N_A^{Wjet}$$

In this procedure the normalization are retrieved, subtracting the SMEW bkg and takes into account the leakage of signal in the bkg regions. The normalization are taken in the region $P_{\tau}(\gamma) < 40$ GeV

Shapes:

- Taken in region C and C'.

For Z+gamma the procedure is the same, except that only the Z+jets bkg is estimated from data.

Fiducial volume

Cuts	$pp \rightarrow l\nu\gamma$	$pp \rightarrow l^+l^-\gamma$	$pp \rightarrow \nu\bar{\nu}\gamma$
Lepton	$p_T^\ell > 25 \text{ GeV}$ $ \eta_\ell < 2.47$ $N_\ell = 1$ $p_T^\nu > 35 \text{ GeV}$	$p_T^\ell > 25 \text{ GeV}$ $ \eta_\ell < 2.47$ $N_{\ell^+} = 1, N_{\ell^-} = 1$ —	— — $N_\ell = 0$ —
Boson	—	$m_{\ell^+\ell^-} > 40 \text{ GeV}$	$p_T^{\nu\nu} > 90 \text{ GeV}$
Photon	$E_T^\gamma > 15 \text{ GeV}$	$E_T^\gamma > 15 \text{ GeV}$ $ \eta^\gamma < 2.37, \Delta R(\ell, \gamma) > 0.7$ $\epsilon_h^p < 0.5$	$E_T^\gamma > 100 \text{ GeV}$
Jet	$E_T^{\text{jet}} > 30 \text{ GeV}, \eta^{\text{jet}} < 4.4$ $\Delta R(e/\mu/\gamma, \text{jet}) > 0.3$ Inclusive : $N_{\text{jet}} \geq 0$, Exclusive : $N_{\text{jet}} = 0$		

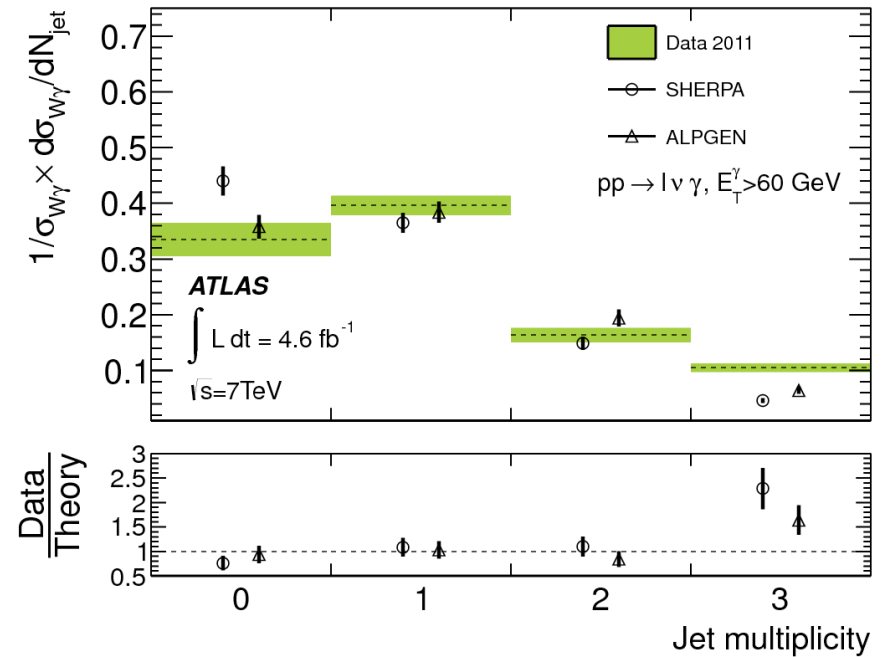
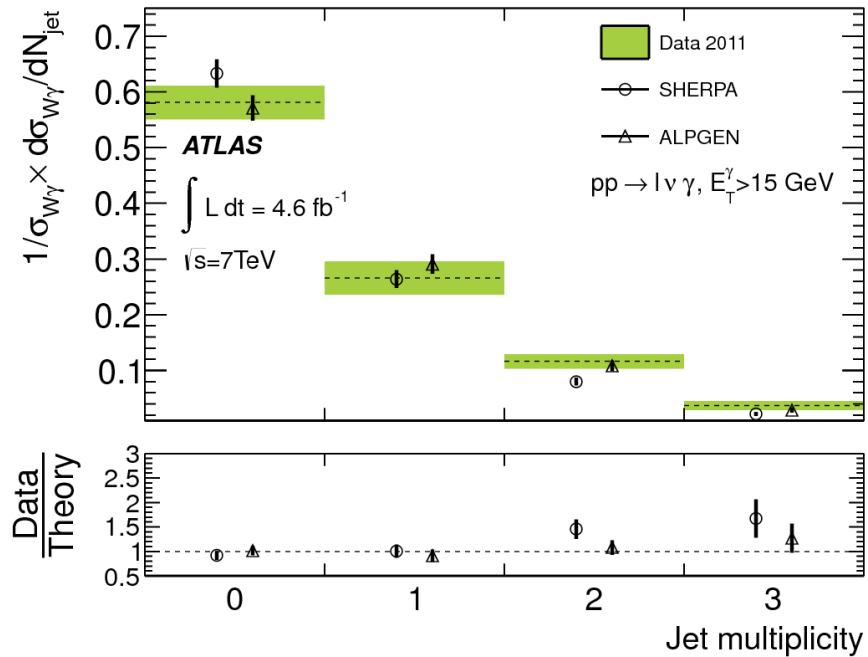
TABLE IV. Definition of the extended fiducial region where the cross sections are evaluated; p_T^ν is the transverse momentum of the neutrino from W decays; $p_T^{\nu\bar{\nu}}$ is the transverse momentum of the Z boson that decays into two neutrinos; N_ℓ is the number of leptons in one event; ϵ_h^p is the photon isolation fraction.

Systematics

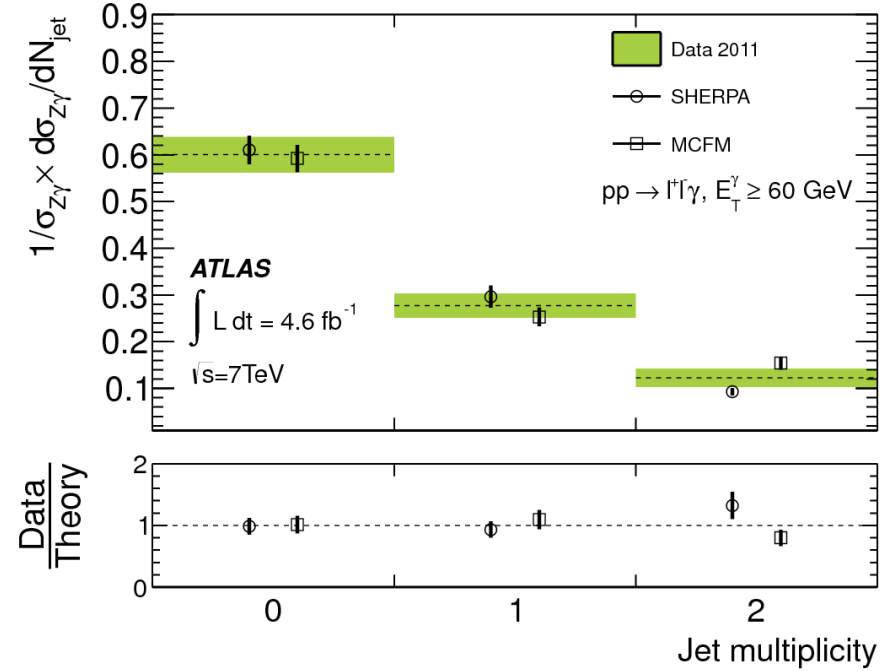
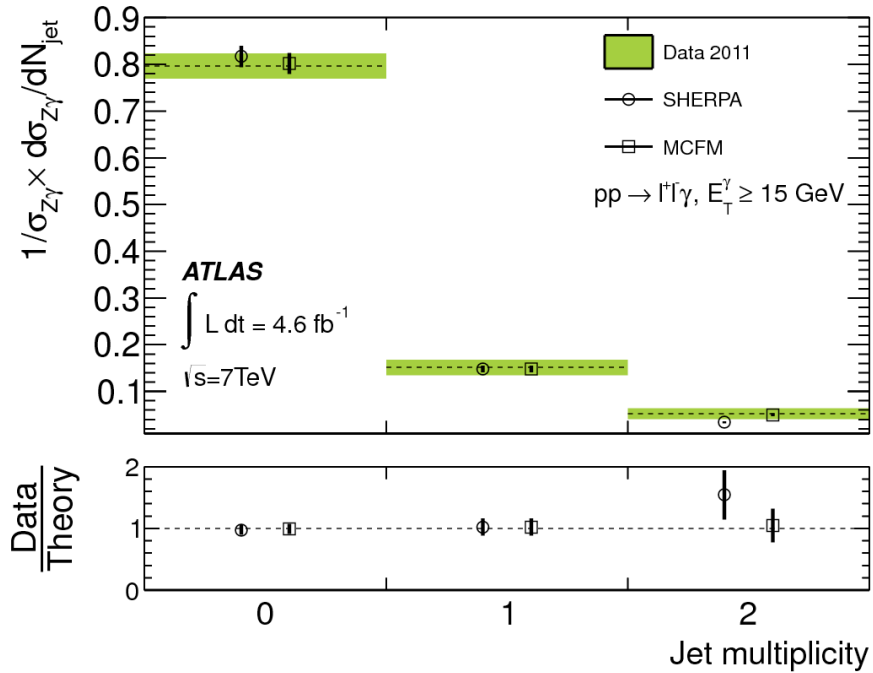
Source	$pp \rightarrow e\nu\gamma$	$pp \rightarrow \mu\nu\gamma$	$pp \rightarrow e^+e^-\gamma$	$pp \rightarrow \mu^+\mu^-\gamma$	$pp \rightarrow \nu\bar{\nu}\gamma$
Relative systematic uncertainties on the signal correction factor $C_{V\gamma}$ [%]					
γ identification efficiency	6.0 (6.0)	6.0 (6.0)	6.0 (6.0)	6.0 (6.0)	5.3 (5.3)
γ isolation efficiency	1.9 (1.8)	1.9 (1.7)	1.4 (1.4)	1.4 (1.4)	2.8 (2.8)
Jet energy scale	0.4 (2.9)	0.4 (3.2)	- (2.2)	- (2.4)	0.6 (2.0)
Jet energy resolution	0.4 (1.5)	0.6 (1.7)	- (1.7)	- (1.8)	0.1 (0.5)
unassociated energy cluster in E_T^{miss}	1.5 (1.6)	0.5 (1.0)	- (-)	- (-)	0.3 (0.2)
μ momentum scale and resolution	- (-)	0.5 (0.4)	- (-)	1.0 (0.8)	- (-)
EM scale and resolution	2.3 (3.0)	1.3 (1.6)	2.8 (2.8)	1.5 (1.5)	2.6 (2.7)
Lepton identification efficiency	1.5 (1.6)	0.4 (0.4)	2.9 (2.5)	0.8 (0.8)	- (-)
Lepton isolation efficiency	0.8 (0.8)	0.3 (0.2)	2.0 (1.6)	0.5 (0.4)	- (-)
Trigger efficiency	0.8 (0.1)	2.2 (2.1)	0.1 (0.1)	0.6 (0.6)	1.0 (1.0)
Total	7.1 (8.0)	6.8 (7.8)	7.6 (7.9)	6.5 (7.1)	6.6 (7.0)

TABLE VI. Relative systematic uncertainties on the signal correction factor $C_{V\gamma}$ for each channel in the inclusive $N_{\text{jet}} \geq 0$ (exclusive $N_{\text{jet}} = 0$) $V\gamma$ measurement.

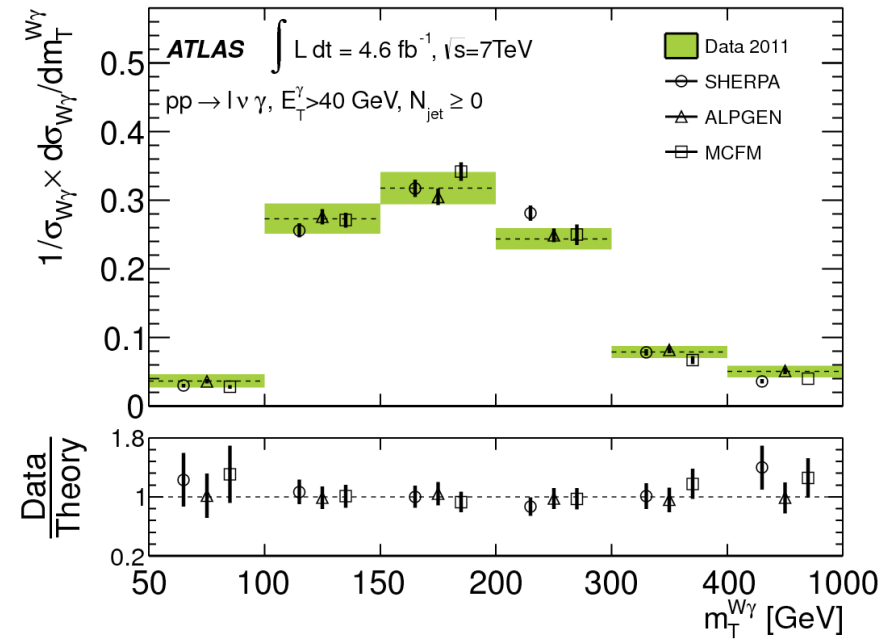
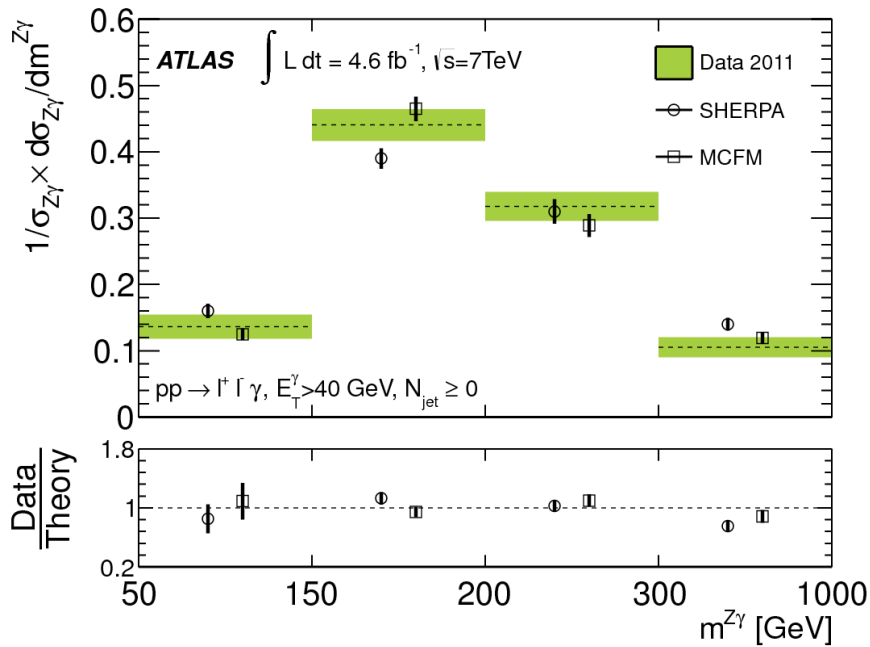
Unfolded jet multiplicity $W(l \nu) \gamma$



Unfolded jet multiplicity $Z(l\ell)\gamma$



Mass Spectrum



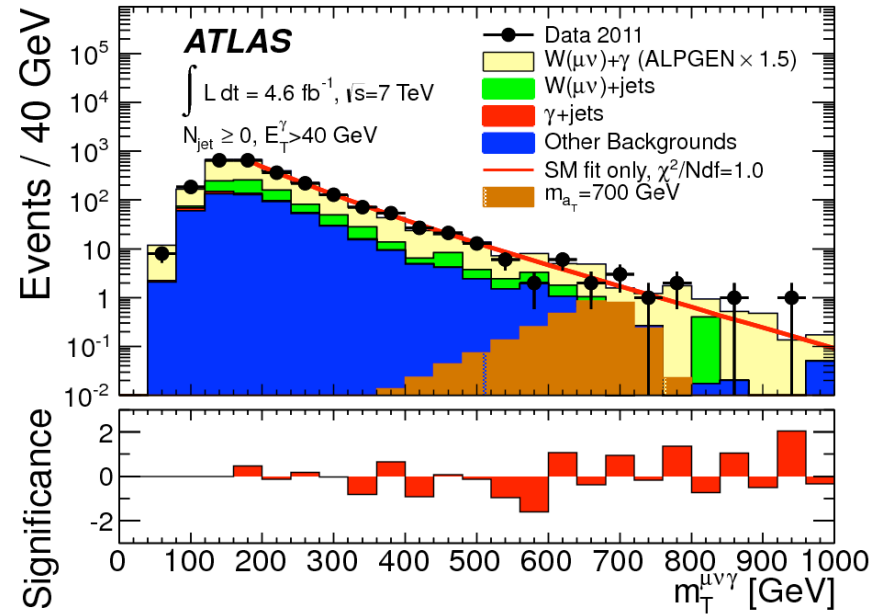
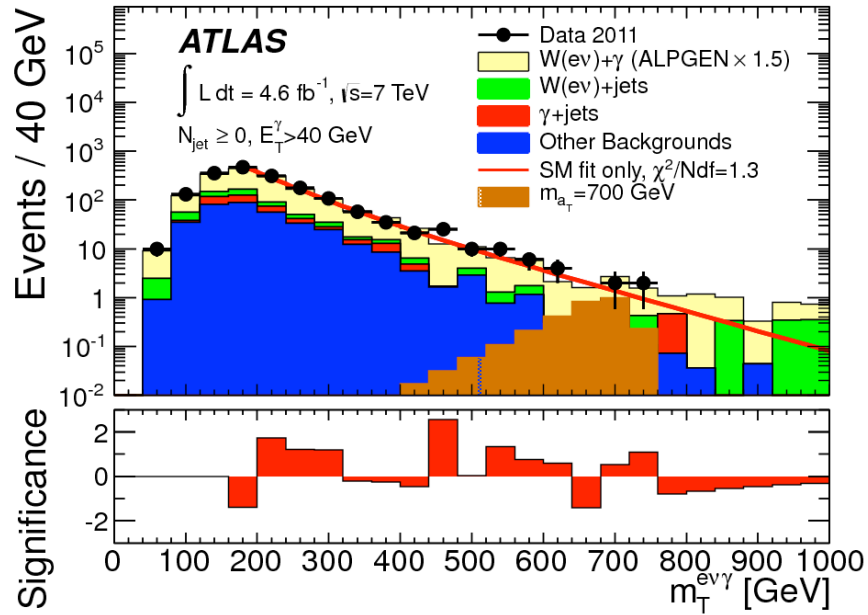
$$\begin{aligned}
 (m_T^{W\gamma})^2 &= \left(\sqrt{m_{\ell\gamma}^2 + |\vec{p}_T(\gamma) + \vec{p}_T(\ell)|^2} + E_T^{\text{miss}} \right)^2 \\
 &\quad - |\vec{p}_T(\gamma) + \vec{p}_T(\ell) + \vec{E}_T^{\text{miss}}|^2.
 \end{aligned}$$

aTGC

processes	Measured	Expected
	$pp \rightarrow \ell\nu\gamma$	
Λ	∞	∞
$\Delta\kappa_\gamma$	(-0.41, 0.46)	(-0.38, 0.43)
λ_γ	(-0.065, 0.061)	(-0.060, 0.056)
Λ	6 TeV	6 TeV
$\Delta\kappa_\gamma$	(-0.41, 0.47)	(-0.38, 0.43)
λ_γ	(-0.068, 0.063)	(-0.063, 0.059)
processes	$pp \rightarrow \nu\nu\gamma$ and $pp \rightarrow \ell^+\ell^-\gamma$	
Λ	∞	∞
h_3^γ	(-0.015, 0.016)	(-0.017, 0.018)
h_3^Z	(-0.013, 0.014)	(-0.015, 0.016)
h_4^γ	(-0.000094, 0.000092)	(-0.00010, 0.00010)
h_4^Z	(-0.000087, 0.000087)	(-0.000097, 0.000097)
Λ	3 TeV	3 TeV
h_3^γ	(-0.023, 0.024)	(-0.027, 0.028)
h_3^Z	(-0.018, 0.020)	(-0.022, 0.024)
h_4^γ	(-0.00037, 0.00036)	(-0.00043, 0.00042)
h_4^Z	(-0.00031, 0.00031)	(-0.00037, 0.00036)

coupling	parameters	channel
$WW\gamma$	$\lambda_\gamma, \Delta\kappa_\gamma$	$WW, W\gamma$
WWZ	$\lambda_Z, \Delta\kappa_Z, \Delta g_1^Z$	WW, WZ
$ZZ\gamma$	h_3^Z, h_4^Z	$Z\gamma$
$Z\gamma\gamma$	h_3^γ, h_4^γ	$Z\gamma$
$Z\gamma Z$	f_{40}^Z, f_{50}^Z	ZZ
ZZZ	$f_{40}^\gamma, f_{50}^\gamma$	ZZ

Search $W(l\nu)\gamma$



Search $Z(\ell\ell)\gamma$

